DOE/PC/95224--T3

TITLE: *IN SITU* INFRARED STUDY OF CATALYTIC DECOMPOSITION OF NO

REPORT TYPE: Semiannually Technical Progress Report

REPORTING PERIOD: August 1, 1996 to February 1, ~~1996~~ 1997

PRINCIPAL AUTHOR(s): Steven S. C. Chuang and Cher-Dip Tan

ISSUED REPORT DATE: April 8, 1997

INSTITUTION: The University of Akron
Department of Chemical Engineering
Akron, Ohio 44325-3906
(330) 972-6993

DOE AWARD NUMBER.: DE-FG22-95PC95224

Disclaimer

Abstract

The growing concerns for the environment and increasingly stringent standards for NO emission have presented a major challenge to control NO emissions from electric utility plants and automobiles. Catalytic decomposition of NO is the most attractive approach for the control of NO emission for its simplicity. Successful development of an effective catalyst for NO decomposition will greatly decrease the equipment and operation cost of NO control. Due to lack of understanding of the mechanism of NO decomposition, efforts on the search of an effective catalyst have been unsuccessful.

Scientific development of an effective catalyst requires fundamental understanding of the nature of active site, the rate-limiting step, and an approach to prolong the life of the catalyst. Research is proposed to study the reactivity of adsorbates for the direct NO decomposition and to investigate the feasibility of two novel approaches for improving catalyst activity and resistance to sintering. The first approach is the use of silanation to stabilize metal crystallites and supports for Cu-ZSM-5 and promoted Pt catalysts; the second is utilization of oxygen spillover and desorption to enhance NO decomposition activity. An innovative infrared reactor system will be used to observe and determine the dynamic behavior and the reactivity of adsorbates during NO decomposition, oxygen spillover, and silanation. A series of experiment including X-ray diffraction, temperature programmed desorption, temperature programmed reaction, X-ray photoelectron spectroscopy will be used to characterize the catalysts. The information obtained from this study will provide a scientific basis for developing an effective catalyst for the NO decomposition under practical flue gas conditions.

Table of Contents

List of Graphical Materials

Executive Summary

During the third semi-annual period, two major tasks were accomplished.

(i) A water and oxygen injection system was built to study the effect of water and oxygen on the NO decomposition catalyst. An effective catalyst for removal of NO_x from stationary sources has to work in the exhaust effluent containing oxygen and 10% steam.

(ii) The effectiveness of silantion on the stability of the catalyst was tested. It was found that silanation slightly deactivate the catalyst and did not provide significant beneficial effect to improve the catalyst performance.

Work is currently underway to determine the mechanism of oxygen spillover and the effect of SO_2 on the catalyst activity for NO decomposition.

In Situ Infrared Study of Catalytic Decomposition of NO

Rhodium is a major component in the automobile three-way catalytic converters which allow simultaneous conversion of three pollutants (i.e., NO, CO, and hydrocarbons) to CO_2 and N_2. The principal function of Rh is to catalyze the reaction of NO with CO to form N_2 and CO_2. The high cost of Rh, the narrow operating window for air/fuel ratio, and increasingly strict standards for NO_x emission have promoted extensive research to develop substitutes for the Rh-based catalyst and to improve the Rh catalyst performance. One critical technical issue related to catalyst performance is the catalyst durability (i.e., the resistance to deactivation). The major causes of deactivation of rhodium in the three-way catalytic converter are the loss of active sites by (a) Rh crystallite sinking into subsurface of γ-Al_2O_3, the major component in the washcoat, at temperatures above 873 K; (b) sintering, resulting from Rh crystallite agglomeration, (c) possible transformation of active Rh^o sites to less active Rh^+ sites, and (d) poisoning.

Zirconia and α-alumina have been found to be effective in inhibiting subsurface penetration of the Rh particle. Sintering of Rh crystallites has been impeded by addition of ceria and stabilization of γ-Al_2O_3 by SiO_2, BaO, and La_2O_3. Ceria also provides a number of beneficial effects to increase the overall efficiency of the three-way catalysts, including stabilization of γ-Al_2O_3, oxygen storage, and promotion of water-gas shift reaction.

Since reduced Rh (Rh^o) site has been found to be more active than the oxidized (Rh^+) site for NO-CO reaction, suppression of the transformation of Rh^o sites to less active Rh^+ sites allow maintenance of high activity for NO reduction. It has been suggested that removal of OH from the γ-Al_2O_3 support by alkylhalosilane may inhibit the transformation of Rh^o sites to Rh^+ sites.

Poisoning of the three-way catalyst is due to irreversible adsorption of SO_2, combustion products of fuel additives, and lubricative additives. One approach to slow down poisoning is to deposit Rh at the end of the pore so that the poison species may adsorb in the outer rhodium-free shell of support which serves as a guard, thus increasing the durability of the catalyst. Species such as NiO has also been added to the catalyst to chemisorb poisons such as SO_2, thus hindering

sulfur poisoning.

While a fuel additive such as tetraethyl lead has long been known to poison the Rh catalysts, the effect of additive such as methylcyclopentadienyl manganese (MMT) on the catalytic converter has been a controversial subject. The most thermodynamic stable form of the combustion products of MMT is MnO which has been known to be the oxophilic promoter. The oxophilic promoter has been found to promote CO dissociation; it may also promote NO dissociation.

The objective of this study is to determine the effect of MnO and silanation on Rh surface states and their activity and selectivity for NO-CO reaction. 4 wt% Rh/SiO_2, $Mn\text{-}Rh/SiO_2$, and trimethychorosilane $[(CH_3)_3SiCl]$- treated Rh/SiO_2 were studied by *in situ* infrared spectroscopy (IR) coupled with temperature-programmed reaction (TPR). Rapid response of the product formation and adsorbates to change in reactant concentration as well as the close match between the IR spectra at the specific temperature during TPR and those during steady-state NO-CO reaction at the same temperature suggest that IR-TPR is an efficient approach to rapidly scan IR spectra of adsorbate under wide range of reaction conditions. Changes in Rh surface state with Mn and silane additives as well as temperature and reactant ratio were determined by *in situ* infrared spectroscopy (IR) of adsorbed CO and NO during reaction.

Results

The 4 wt% Rh/SiO_2 catalyst was prepared by incipient wetness impregnation of large pore SiO_2 (Strem, 300 m^2/g) support with $RhCl_3 \cdot 3H_2O$ (Alfa Chemicals) solution. The ratio of the solution to the weight of support material used was 1 cm^3 to 1 g. After impregnation, the catalyst sample was dried overnight in air at 303 K and reduced in a flow of hydrogen at 673 K for 16 h. The H_2 uptake of the catalyst was measured at 303 K by pulse adsorption method and was found to be 61 μmol/g, corresponding to a dispersion of 0.62 and a crystallite size of 15 Å based on adsorption stoichiometry of $H_{ads}/Rh = 1$ and a cubic shape of Rh crystallites. The $Mn\text{-}Rh/SiO_2$ catalyst was prepared by sequential impregnation of the unmodified Rh/SiO_2 catalyst with an aqueous solution of $Mn(NO_3)_2 \cdot 6H_2O$ (Mn/Rh=0.1). The sample was dried at 298 K overnight

and further reduced at 673 K for 16 h. The hydrogen uptake of Mn-Rh/SiO_2 was 57 μmol/g, corresponding to a dispersion of Rh metal of 0.57. The addition of Mn showed a minimal effect on hydrogen uptake. This result is consistent with the literature that the addition of Mn did not significantly influence the amount of H_2 chemisorption at room temperature.

The silane modified 4 wt% Rh/SiO_2 catalyst was prepared by preadsorbed CO and followed by injection of a known quantity (1 cm^3) of trimethychlorosilane [$(CH_3)_3SiCl$] vapor into the IR reactor cell in flowing Helium at 323 K. The added $(CH_3)_3SiCl$ caused a significant decrease in the intensity of OH group at 3744 cm^{-1}, confirming the occurrence of silanization. Following the silanization, the catalyst was reduced in hydrogen at 573 K to remove methyl ligand at 2965 cm^{-1} and Cl.

TPR-IR studies were carried out in an *in situ* infrared (IR) reactor cell with CaF_2 windows capable of operating upto 873 K and 6 MPa. The detailed description of the apparatus and experimental procedures used in this study has been reported elsewhere and is briefly described here. The reactant gases used are CO (Linde, Commercial Grade), NO, and He (Linde, UHP); the gas flows were controlled by Brooks 5850E mass flow controllers. Helium, an inert gas in the reaction, was used to keep a low concentration of the ionized species in the MS vacuum chamber for high sensitivity to reaction products. The catalyst was reduced at 673 K for 1 h prior to the TPR-IR studies. The reactant mixture with a specific NO:CO:He ratio entered the IR cell at a constant flow rate while the catalyst in the IR cell was heated at 10 K/min. The change in the concentration of adsorbates was monitored by a Nicolet 5SXC infrared spectrometer with a DTGS detector at a resolution of 4 cm^{-1}. The gaseous composition of the reactor effluents were monitored using a Balzers QMG 112 quadrupole mass spectrometer (MS). The *m/e* ratios followed by the MS were 2 for He, 28 for CO/N_2, 30 for NO, 44 for CO_2/N_2O, 46 for NO_2, and 22 for the secondary ionization of CO_2. It should be noted that N_2 and CO give the same mass-to-charge ratio (*m/e*) of 28. The absence of the secondary ionization does not allow the separation of these two species.

NO-CO Reaction over Rh/SiO_2. Figure 1(a) shows infrared spectra of adsorbates on 4 wt% Rh/SiO_2 catalyst during the TPR of NO-CO at a ratio of 1:1. The adsorbates observed for TPR are the low wavenumber Rh-NO^- at 1698 cm^{-1}, high wavenumber Rh-NO^- at 1755 cm^{-1}, cationic NO [Rh-NO^+] at 1916 cm^{-1}, gem-dicarbonyl CO [$Rh^+(CO)_2$ at 2088 and 2033 cm^{-1}, linear CO [Rh-CO] at 2055 cm^{-1}, linear CO on Rh^+ site [$Rh^+(CO)$] at 2100 cm^{-1}, isocyanate on Rh metal [Rh-NCO] at 2188 cm^{-1}, and isocyanate on SiO_2 support [Si-NCO] at 2294 cm^{-1}. The difference between the low wavenumber and the high wavenumber Rh-NO^- has been attributed to the different extent of electron back donation from the reduced Rh site to adsorbed NO. The mode of NO and CO adsorbates and their intensities show strong temperature dependence which can be divided into three temperature regimes: (i) the 303 K - 403 K region where the conversion of reactants is low, (ii) the 413 K - 563 K region where appreciable conversion occurred, and (iii) above 563 K, the light-off temperature. These different temperature regions give the distinct difference in both intensity and the form of adsorbates.

In the 303 - 403 K region, the low wavenumber (LW) Rh-NO^- species at 1698 cm^{-1} is the predominant adsorbate. Increase in temperature increased the intensity of LW Rh-NO^- with a red shift (decrease in the wavenumber). The variation of intensity and wavenumber of the species are plotted in Fig 1 (b). The corresponding MS analysis (Fig. 2 (a)) of the NO and NO TOF (Fig. 2 (b)) show that NO conversion is below .

In the 403 - 563 K region, the product formation and NO conversion increased, as shown in Figs. 2 (a) and (b). The increase in NO conversion and products formation were accompanied with the change in mode of adsorbates and their intensities. The concomitant disappearance of HW Rh-NO^- and the increase in intensities of $Rh^+(CO)_2$ and Rh-NO^+ suggests that oxygen resulted from the dissociation of HW Rh-NO^- converted Rh^o to Rh^+ (i.e., oxidative disruption), which have also been observed during pulse NO-CO reaction studies over Rh/SiO_2 and Rh/Al_2O_3 catalysts. The absorbance intensity of $Rh^+(CO)_2$ as a function of temperature, plotted in Figure 1 (b) shows that $Rh^+(CO)_2$ intensity increased to its maximum at 473 K and decreased. The absence of significant variation of LW Rh-NO- suggest that the reduced Rh site for the adsorbates remains

nearly constant below the lightoff temperature. The appearance of Rh-NCO and the increase in Si-NCO intensity with temperature reveals that NCO is migrated from Rh site to SiO_2 site.

A major change in adsorbate intensity is observed at 563 - 573 K where lightoff occurred. All the NO and CO adsorbates show a dramatic decrease to near zero coverage while gaseous CO_2 bands at 2361 and 2330 cm^{-1} and Si-NCO increased to a constant density. The MS analysis shown in Fig. 2 (a) reveals that the lightoff took place at 573 K where 50% NO conversion is achieved. The sharp increase in product formation and NO conversion appears to be due to the heat effect on the rate of NO-CO reaction. The catalyst support temperature measured by intensity of SiO_2 overtone is 637 K while the temperature of gaseous reactant measured by thermocouple is 573 K. The significant temperature difference between catalyst support (T_s) and gas phase (T_s) as shown in Fig. 3 (a) reveals that heat released from reaction caused a rapid temperature rise, resulting a sharp increase in reaction rate. Assuming the activation energy did not vary before and after lightoff, extrapolation the TOF for NO conversion to higher temperature show the nonisothermal effectiveness factor is 5 at the light-off and 1.2 above the lightoff at 673 K.

NO-CO TPR experiment under various NO/CO ratios was also conducted to determine the effect of partial pressure of reactants on the structure adsorbates and catalyst surface state. The reactant ratio NO to CO = 1:5 in Fig. 1 (c) resemble the CO/NO ratio in the typical exhaust of an automobile engine. Figs. 1 (a), (c) and (e) show that LW Rh-NO^-, $Rh^+(CO)_2$, and $Rh^+(CO)$ were the major adsorbates observed below light-off temperatures and were completely disappeared above light-off temperatures.

Comparison of Figs. 1 (c) and (d) with (a) and (b) reveals that increasing in CO partial pressure caused (i) increase in linear CO [Rh-CO] at 2055 cm^{-1} in 303 - 413 K range, (ii) decrease in HW Rh-NO^- and LW Rh-NO^- in the 413 - 563 K region, and (iii) lowering $Rh^+(CO)_2$ intensity shifting its maximum intensity to 523 K. Above light-off temperature, incising in CO partial caused significant increase in both Rh-NCO and Si-NCO intensity and the formation of linear CO on the reduced Rh. The formation of Rh-CO is resulted from the reductive agglomeration of Rh^+ to Rh^o.

Fig. 1 (e) shows that high NO partial pressure resulted in: (i) formation of a neutral NO [Rh-NO^{o}] at 1855 cm^{-1} in the low conversion region between 303 and 413 K, (ii) formation and growth of two bands at 1761 and 1822 cm^{-1} starting at 373 and 463 K, respectively, in the 413 - 563 K region. The bands are having the same intensity at 493 K and are unequivocally assigned to HW Rh-NO^{-} and neutral Rh-NO, respectively. The vibrational frequencies also coincide with the IR spectra of gem-dinitrosyl [Rh^{+}(NO)$_2$] which was observed on Rh^{+} site on Rh/Al_2O_3 and Rh-Y zeolite [15,16]. The intensities of Rh-NO^{+}, Rh-NO, and HW Rh-NO^{-} bands decreased above 493 K. The intensity of LW Rh-NO^{-}, remaining largely unchanged below 493 K, increased and completely disappeared above 583 K. Above 563 K, linear CO was not observed. In addition, isocyanate species were not observed both in the 413 - 563 K region and above 563 K, indicating that excess NO probably inhibited NCO formation.

NO-CO Reaction over MnO Modified Rh/SiO_2. TPR results obtained for the NO-CO reaction over MnO modified Rh/SiO_2 under various NO/CO ratios are presented in Figs. 4 and 5. In the 303 - 413 K region, Fig. 4 (a) shows two shoulder bands at 1615 and 1731 cm^{-1} which were not observed under the same condition (NO/CO = 1) on Rh/SiO_2 (Fig. 1 (a)). The bands are remained to be assigned. In the 413 - 563 K region, the formation of Rh^{+}(CO) and Rh^{+}(CO)$_2$ on the Mn-Rh/SiO_2 begins at 453 K which is at a higher temperature compared to that on the Rh/SiO_2 at 413 K under the same condition.

Fig. 4 (c) shows the formation of Rh-CO at 2060 cm^{-1} at NO/CO = 0.2, indicating higher ratio of CO to NO kept the catalyst surface at a reduced state in the 303 - 413 K region. Fig. 4 (c) also shows that LW Rh-NO^{-} is the only adsorbed NO which is in contrast to the case on Rh/SiO_2 that Rh-NO^{o} and HW Rh-NO^{-} are also observed in the 413 - 563 K region. The absence of HW Rh-NO^{-} together with the low intensities of Rh^{+}(CO)$_2$, and with LW Rh-NO^{-} as the predominant adsorbed NO on Mn-Rh/SiO_2 at all NO/CO ratios, suggest that adding Mn to Rh/SiO_2 resulted in forming large Rh crystallite. In contrast to Rh/SiO_2, the disappearance of Rh^{+}(CO)$_2$ did not accompany the formation of Rh-CO on Mn-Rh/SiO_2 above the light-off temperature.

NO-CO Reaction over Silane Modified Rh/SiO_2. Figs. 6 and 7 shows the IR spectra and MS analysis obtained during the NO-CO (1:1) TPR study on silane modified Rh/SiO_2 catalyst. Careful comparison of Figs. 1 (a), 4 (a), 6 and 7 concludes that silanization of surface OH group did not inhibit the oxidative disruption of Rh^o to Rh^+, as evidenced by the formation of $Rh^+(CO)_2$ and the absence of linear and bridged CO. The intensities of $Rh^+(CO)_2$ are the lowest on silane modified Rh surface compared to those on unmodified and MnO modified Rh/SiO_2. The adsorbed oxygen resulted from the NO dissociation of HW Rh-NO^- at 1755 cm^- oxidized Rh^o to Rh^+ which chemisorbed CO as $Rh^+(CO)_2$. The absence of light-off characteristic during the TPR study suggests that the catalyst might be poisoned by $(CH_3)_3SiCl$.

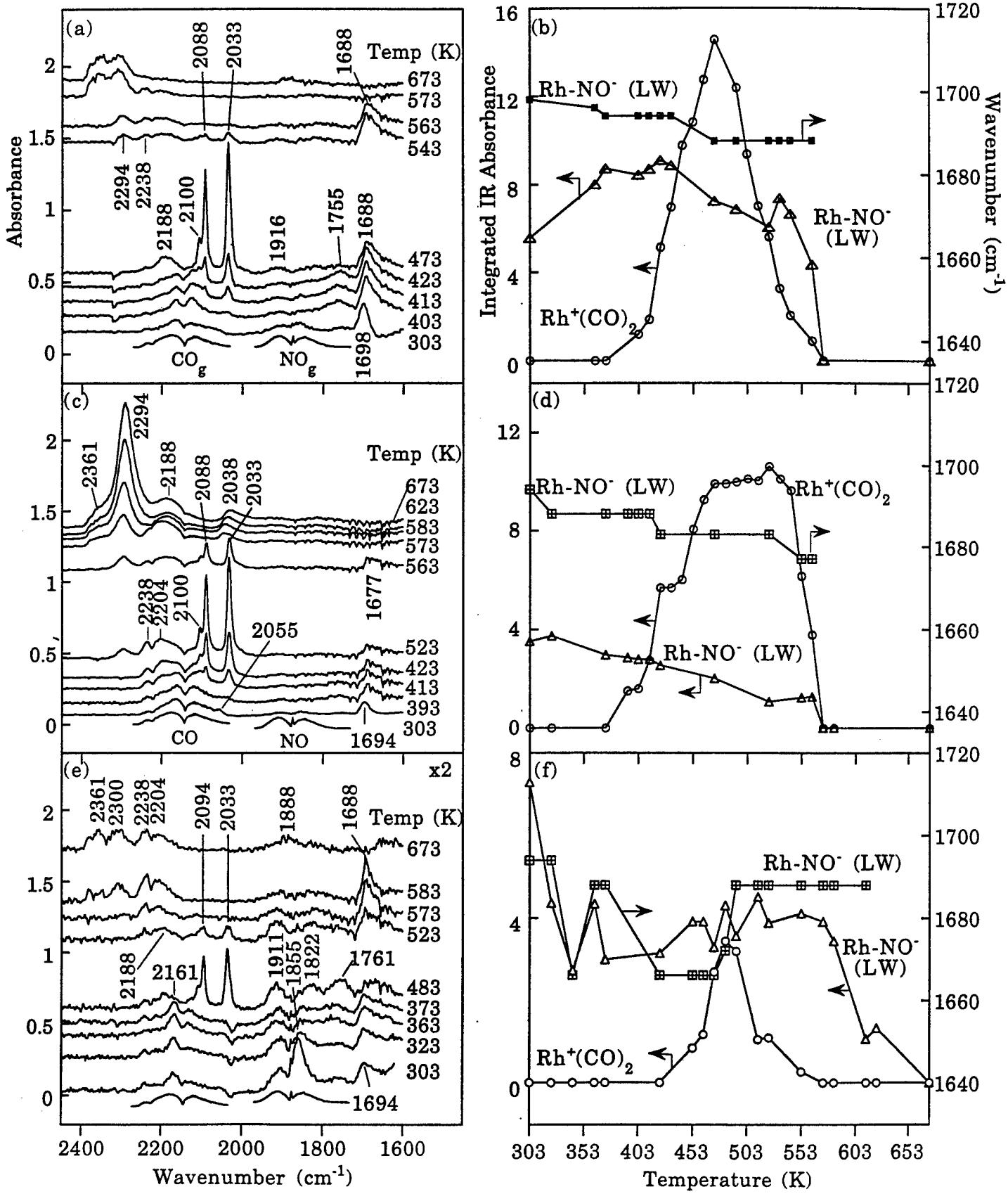
(a)
Temp (K)
673
573
563
543
2088
2033
1688
2294
2238
2188
2100
1916
1755
1688
473
423
413
403
303
CO$_g$
NO$_g$
1698
Absorbance
(b)
Rh-NO$^-$ (LW)
Rh$^+$(CO)$_2$
Rh-NO$^-$ (LW)
Integrated IR Absorbance
Wavenumber (cm^{-1})
(c)
Temp (K)
673
623
583
573
563
2361
2294
2188
2088
2038
2033
1677
2238
2204
2100
2055
523
423
413
393
303
CO
NO
1694
(d)
Rh-NO$^-$ (LW)
Rh$^+$(CO)$_2$
Rh-NO$^-$ (LW)
(e)
x2
Temp (K)
673
583
573
523
2361
2300
2238
2204
2094
2033
1888
1688
2188
2161
1911
1855
1822
1761
483
373
363
323
303
1694
(f)
Rh-NO$^-$ (LW)
Rh-NO$^-$ (LW)
Rh$^+$(CO)$_2$
2400
2200
2000
1800
1600
Wavenumber (cm^{-1})
303
353
403
453
503
553
603
653
Temperature (K)

Fig 1

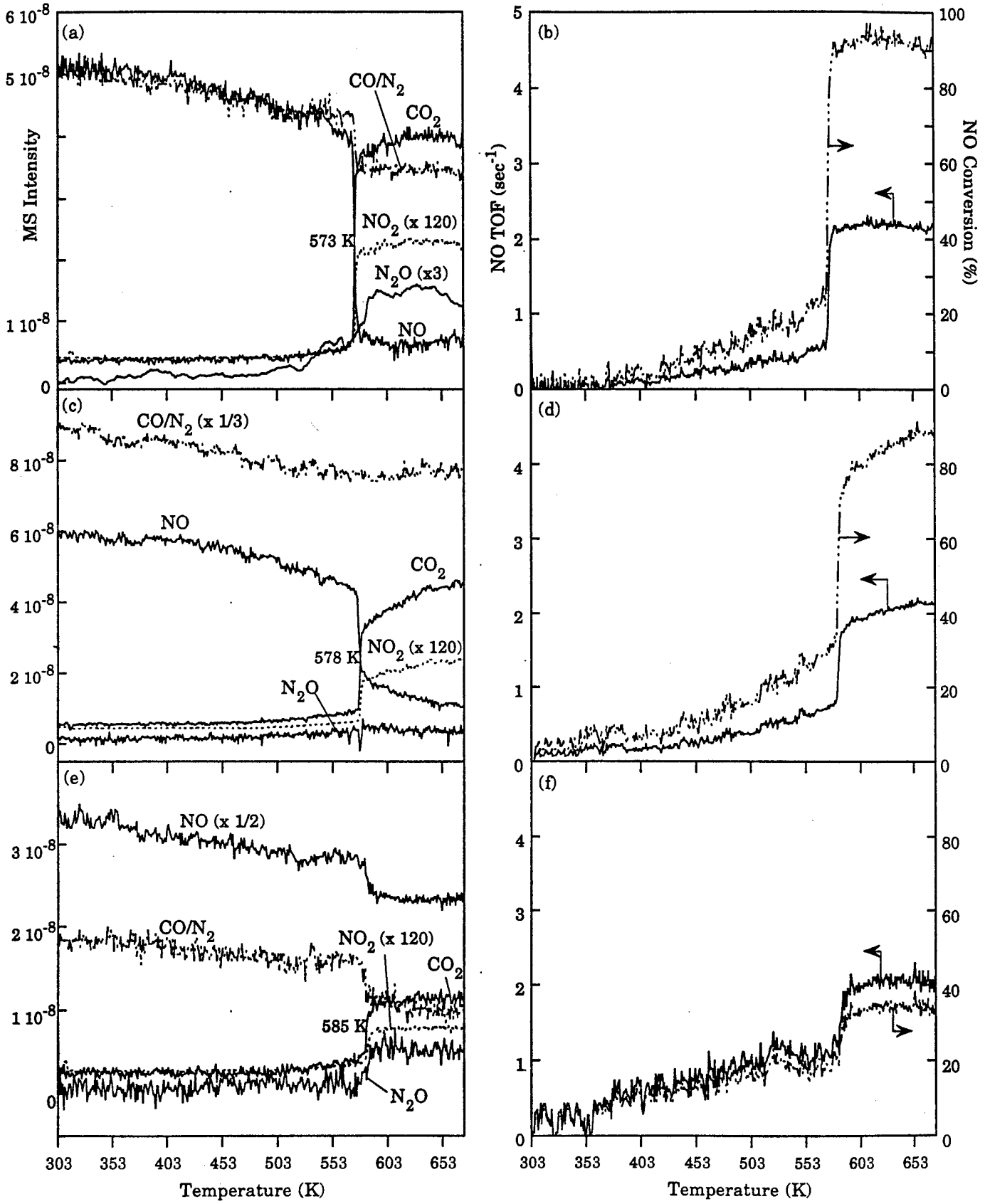
(a)
(b)
(c)
(d)
(e)
(f)
MS Intensity
NO TOF (sec^{-1})
NO Conversion (%)
CO/N$_2$
CO$_2$
NO$_2$ (x 120)
N$_2$O (x3)
NO
573 K
CO/N$_2$ (x 1/3)
NO
CO$_2$
NO$_2$ (x 120)
578 K
N$_2$O
NO (x 1/2)
CO/N$_2$
NO$_2$ (x 120)
CO$_2$
585 K
N$_2$O
Temperature (K)
Temperature (K)

Fig 2

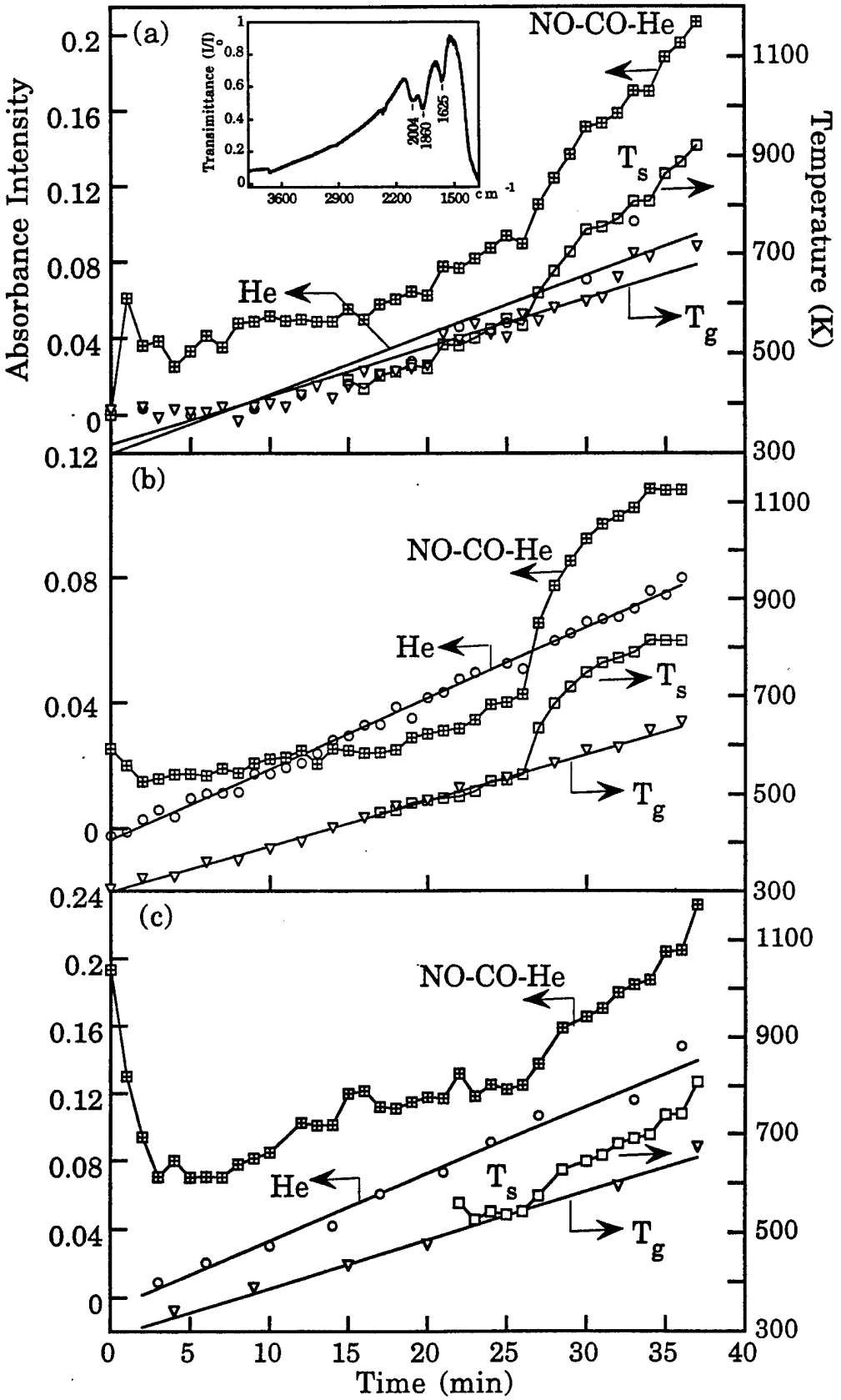
(a)
(b)
(c)
NO-CO-He
He
T_s
T_g
Absorbance Intensity
Temperature (K)
Time (min)
Transmittance (I/I$_o$)
2004
1860
1625
cm^{-1}

Fig 3

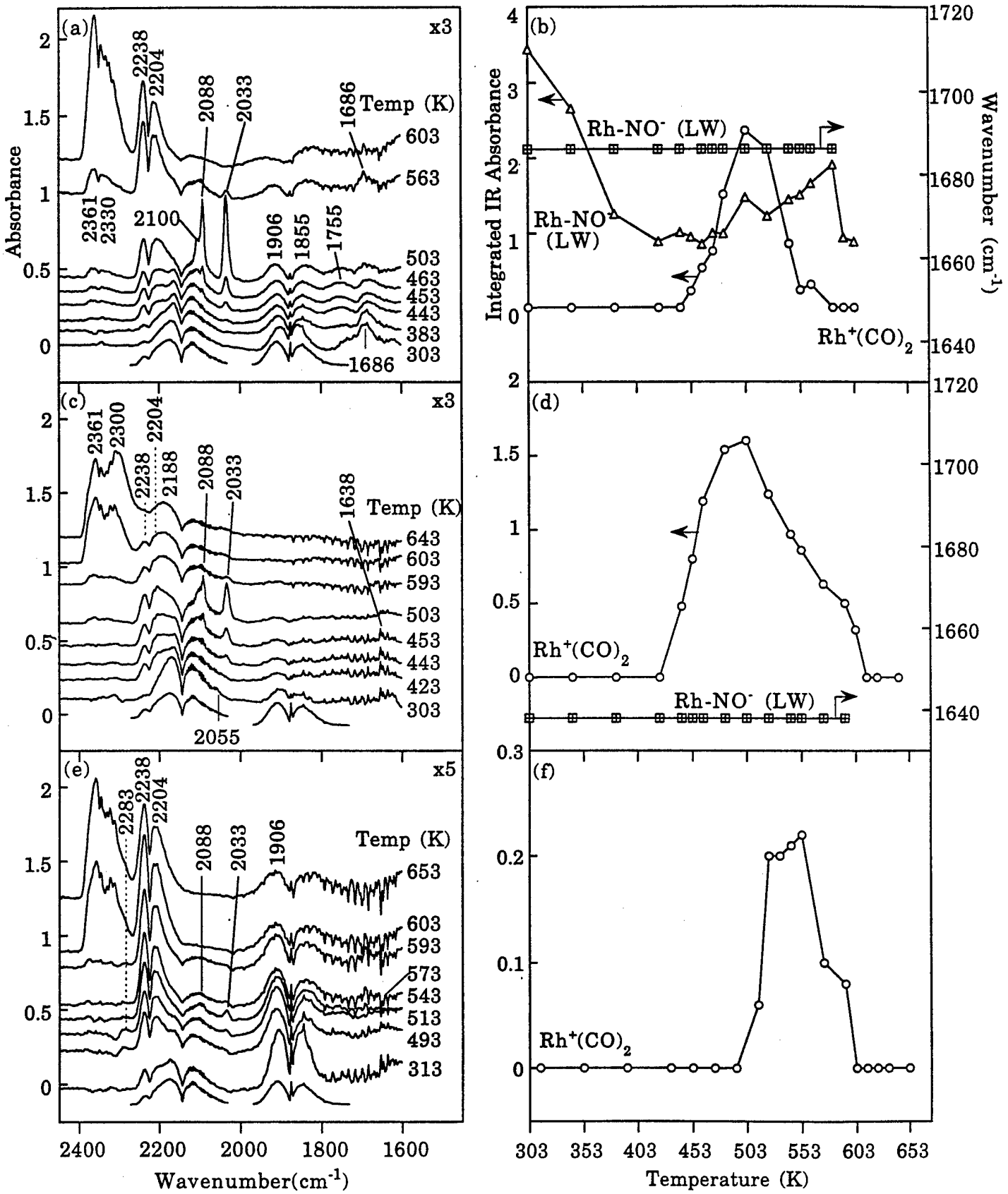
(a)
x3
Absorbance
2238
2204
2088
2033
1686
Temp (K)
603
563
2361
2330
2100
1906
1855
1755
503
463
453
443
383
303
1686
(c)
x3
2361
2300
2204
2238
2188
2088
2033
1638
Temp (K)
643
603
593
503
453
443
423
303
2055
(e)
x5
2283
2238
2204
2088
2033
1906
Temp (K)
653
603
593
573
543
513
493
313
2400
2200
2000
1800
1600
Wavenumber(cm-1)
(b)
Integrated IR Absorbance
Rh-NO- (LW)
Rh-NO- (LW)
Rh+(CO)2
Wavenumber (cm-1)
(d)
Rh+(CO)2
Rh-NO- (LW)
(f)
Rh+(CO)2
303
353
403
453
503
553
603
653
Temperature (K)

Fig 4

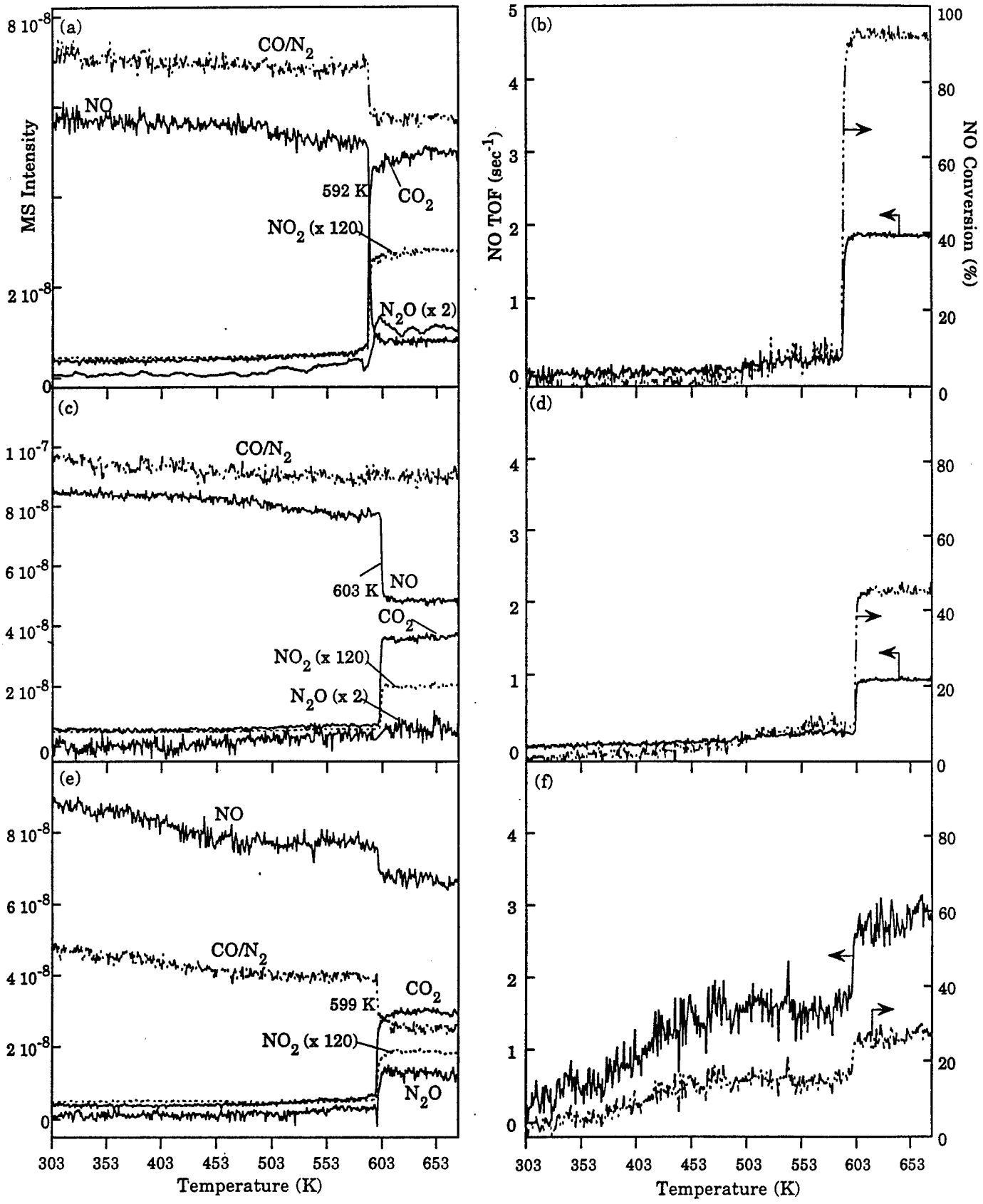
(a)
CO/N2
NO
592 K
CO2
NO2 (x 120)
N2O (x 2)
MS Intensity
8 10-8
2 10-8
0
(b)
NO TOF (sec-1)
NO Conversion (%)
(c)
CO/N2
603 K
NO
CO2
NO2 (x 120)
N2O (x 2)
1 10-7
6 10-8
4 10-8
(d)
(e)
599 K
(f)
303 353 403 453 503 553 603 653
Temperature (K)

Fig 5

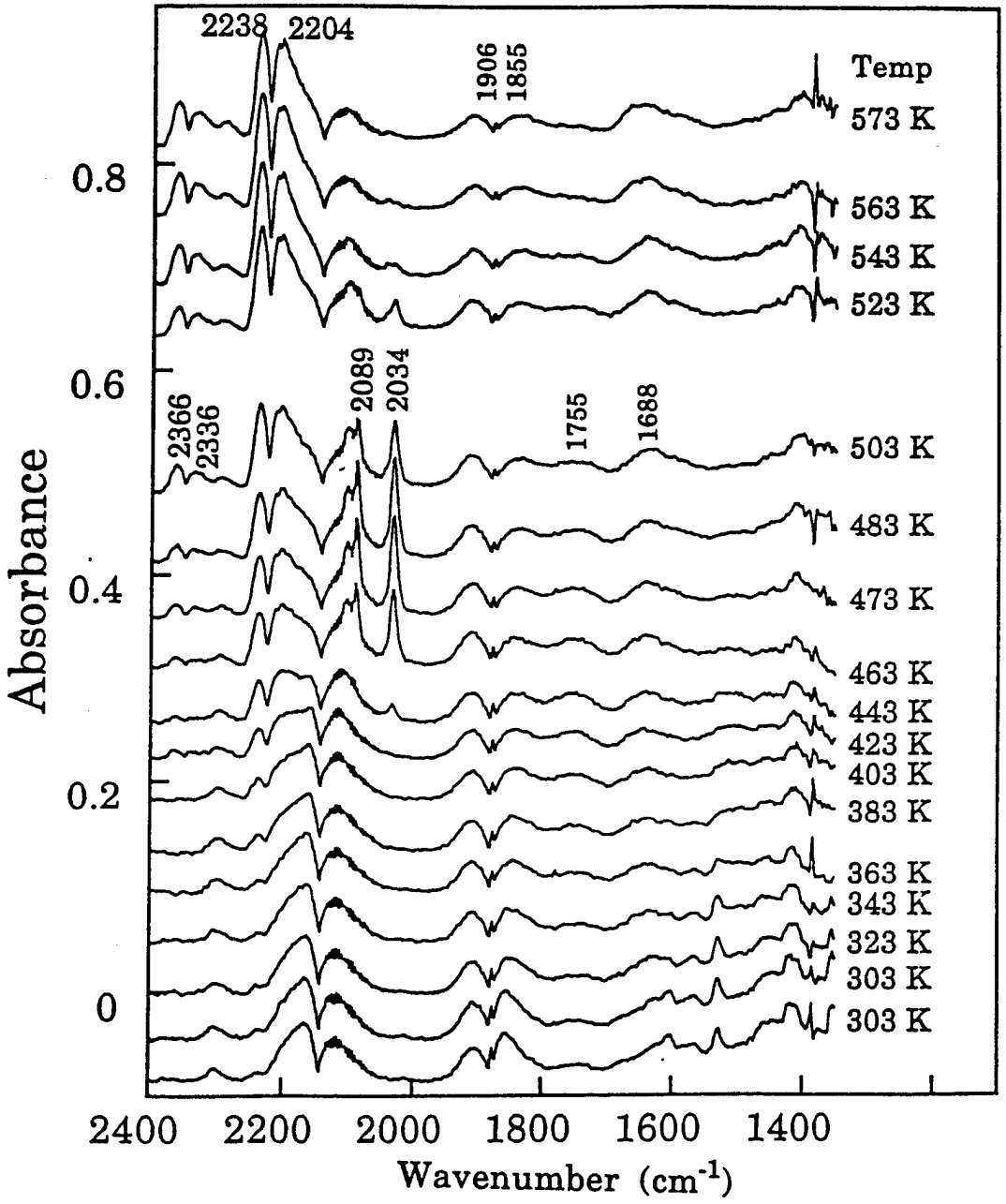
2238
2204
1906
1855
Temp
573 K
563 K
543 K
523 K
2366
2336
2089
2034
1755
1688
503 K
483 K
473 K
463 K
443 K
423 K
403 K
383 K
363 K
343 K
323 K
303 K
303 K
Absorbance
0.8
0.6
0.4
0.2
0
2400
2200
2000
1800
1600
1400
Wavenumber (cm-1)

Fig 6

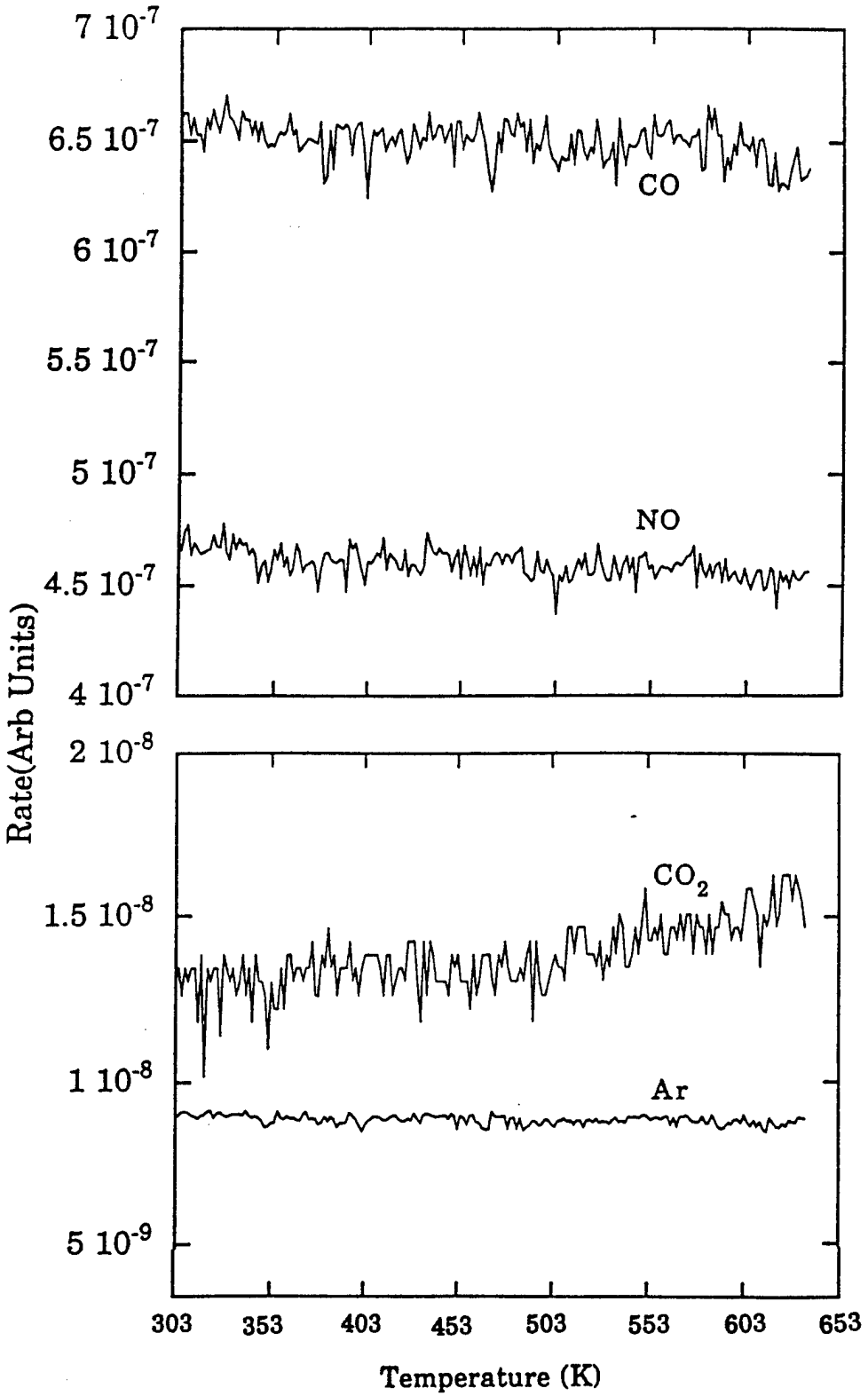
7 10-7
6.5 10-7
6 10-7
5.5 10-7
5 10-7
4.5 10-7
4 10-7
CO
NO
2 10-8
1.5 10-8
1 10-8
5 10-9
CO2
Ar
Rate(Arb Units)
303
353
403
453
503
553
603
653
Temperature (K)

Fig 7

Report Number (14) DOE/PC/95224--T3

Publ. Date (11) 19970408

Sponsor Code (18) DOE/EE, XF

JC Category (19) UC-101, DOE/ER

DOE